Supplement of Earth Syst. Dynam., 11, 563–577, 2020
https://doi.org/10.5194/esd-11-563-2020-supplement

Earth System Dynamics
Open Access
EGU

Supplement of

The role of prior assumptions in carbon budget calculations

Benjamin Sanderson

Correspondence to: Benjamin Sanderson (sanderson@cerfacs.fr)

S1 Prior assumptions on Realized Warming Fraction

The RWF constraint refers to the observation in Millar et al. (2015) that in CMIP5, at least, the TCR and ECS values are well correlated, such that the ratio of the two values $TCR : ECS$ lies between 0.45 and 0.75 throughout the ensemble. This is apparent by considering Figure S2(a), which shows the joint CMIP5 distribution for the two quantities. The consistency of this relationship informed the parameter distribution choice for a pulse-response model ensemble used in Millar et al. (2017c), where a relationship between ECS and TCR was represented in the distribution of plausible models.

However, as is shown in Proistosescu and Huybers (2017) and in Figure S1, for most models in the CMIP5 and CMIP6 ensembles, the constant feedback ECS is likely an underestimate of true equilibrium response to forcing. Fitting a 2-timescale model directly to model output time-series allows the computation of the possible values of equilibrium climate sensitivity consistent with the first 150 years of simulation (Figure S1). In many cases the extrapolated equilibrium temperature is not strongly constrained by the 150 year simulations. However, some features are generally discernible: in most models the uncertainty distribution contains values which are generally greater than the Effective Climate Sensitivity estimate (Gregory et al., 2004).

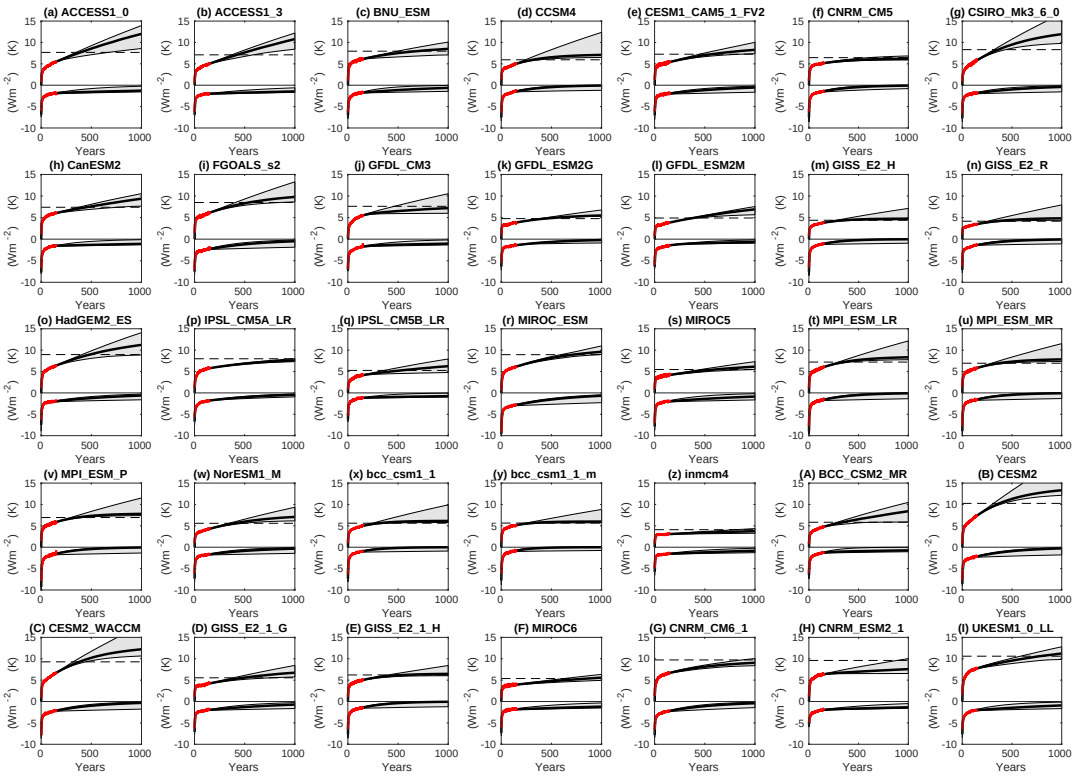

Figure S1. A Figure showing the temperature response to a quadrupling of carbon dioxide. Red points show annual mean temperature from the model's 150 year simulation, the red central line shows the best fitting 2 timescale pulse response model, while the pink area shows the 10th and 90th percentiles of the MCMC distribution of possible pulse response models. The dashed black line shows the Effective climate sensitivity(Gregory et al., 2004).

Figure S2. Black circles show Effective Climate Sensitivity (calculated as a constant feedback extrapolation following Gregory et al. (2004)) as a function of Transient Climate Response (warming at time of CO2 concentration doubling in each model's 1 percent CO2 ramping experiment. Each point shows one model in the CMIP5/6 ensemble, and the circle shows the 5th percentile of the prior joint distribution for ECS and TCR used in Millar et al. (2017c). Red whisker plots show the relationship between TCR and ECS calculated using the 2-timescale pulse-response model fits to the abrupt4xCO2 simulation of the corresponding CMIP5 model.

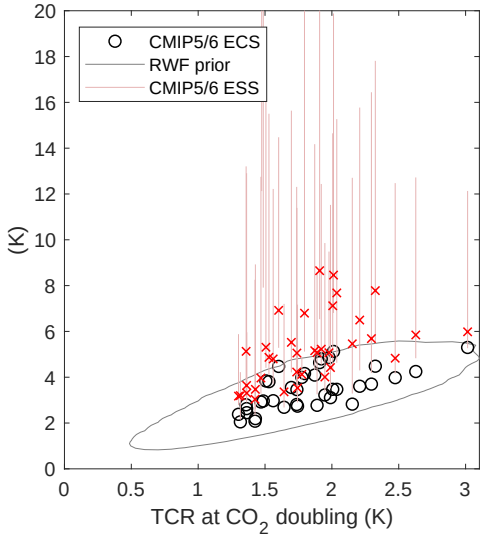

Figure S2 shows EffCS and ECS as a function of TCR for each model in CMIP5 (and some available models in CMIP6). ECS is estimated as in Gregory et al. (2004), while EffCS is calculated by performing an MCMC fit (as in section 1.1.1 using the 150 year global mean surface temperature timeseries of each CMIP5 and CMIP6 model's abrupt4xCO2 simulation to the 2 timescale pulse response model (itself forced by a step function forcing timeseries corresponding to 7.2Wm^{-2} after the first timestep). The resulting posterior distribution of the combined value of q_1 and q_2 then informs the range of plausible values of ECS which are consistent with the CMIP5 or CMIP6 simulation.

It is notable that there is no discernible relationship between possible values of ECS (fitted here with a flat prior allowing values between 0 and 40) and TCR in CMIP5 because the values of ECS are not strongly constrained. As such, there is little basis to assume that the equilibrium sensitivity of the system is well constrained by the TCR in the form of an RWF prior.

S2 Joint distributions of parameters in MCMC optimization

Figures S5, S6, S7 and S8 and show pairwise posterior distributions of the parameters optimized using historical emissions and HadCRUT-CW temperature evolution from 1850-2016 in the 'C.T', 'C,T.H', 'C,T, RWF' and 'C,T,Paleo' constraints respectively.

In all cases, it is apparent that there are a range of solutions allowing for different timescales of response in the pulse-response model which can describe climate evolution to date within the provided constraints. For example, in Figure S5, there is a trade-off between q_2 and d_2 parameters, which represent equilibrium climate response on fast timescales and timescale of the shallow ocean thermal response of the system. There is also a trade-off between the q_2 and q_1 (the component of ECS associated with slow feedbacks associated with warming of the deep ocean component). Introducing a constraint on ocean heat content, at least in this configuration, constrains r_1, the fraction of heat absorbed by the deep ocean - but has only a minor constraining effect on ECS S6.

The 'RWF' cases (Figure S7), however, has a significant effect on ECS. The deep ocean/slow component of ECS (q_1) is constrained to be small by the RWF constraint (which states that 40-60 percent of equilibrium warming associated with current

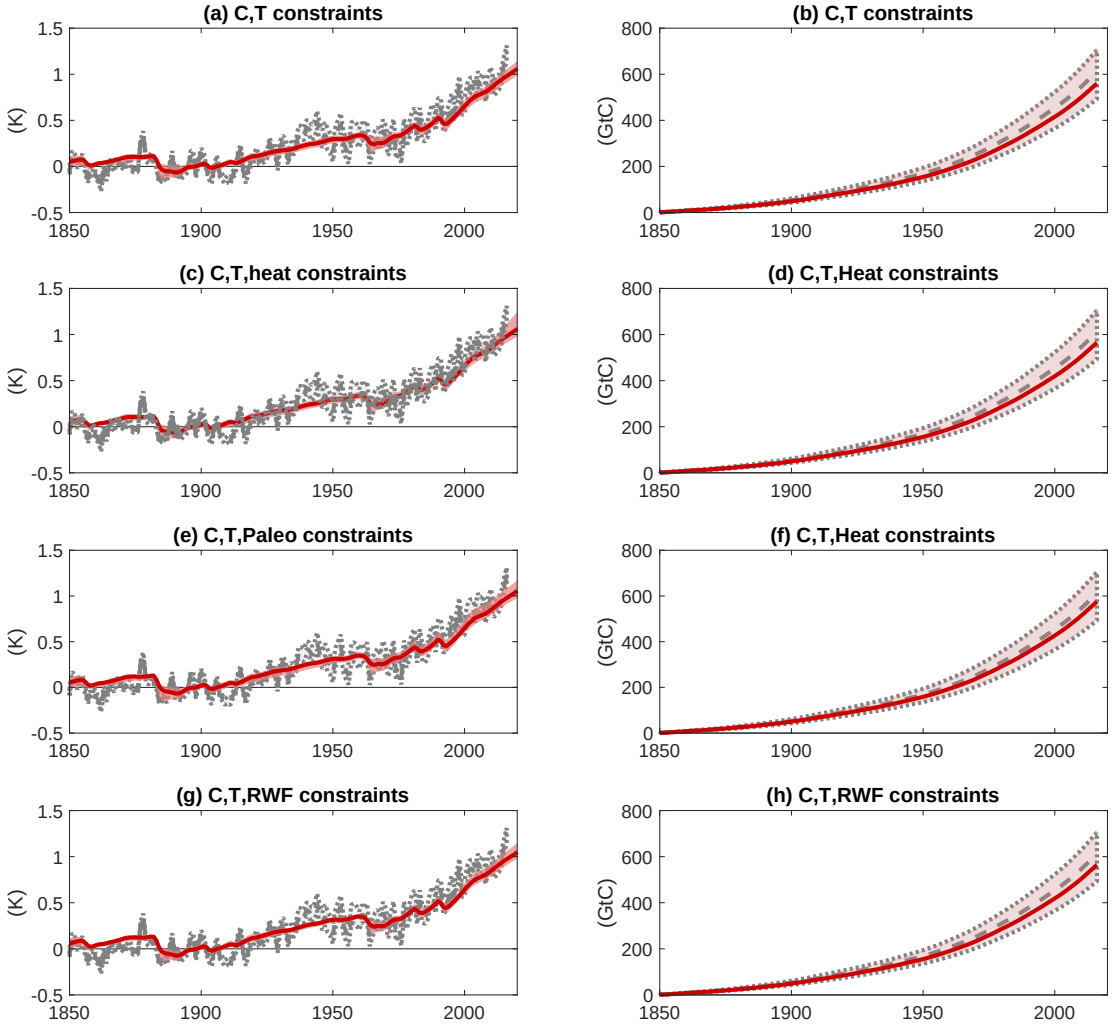

Figure S3. Illustration of ensemble spread (given different prior assumptions) in global mean temperature (a,c,e,g) and cumulative carbon emissions (b,d,f,h) for the observed period. Observational median is grey line, while 5-95% observational uncertain ranges are shown in grey shade (Cowtan and Way (2013) for temperature and Le Quéré et al. (2017); Millar and Friedlingstein (2018) for cumulative emissions). Ensemble median in the historical period is shown in red, with 5-95% ensemble range in red shade.

greenhouse gas concentrations has already been realized). S8) constrain the sum of the 2 equilibrium responses q_n, which is apparent in the parameter distributions by the truncated distribution for q_1 in Figure S8 and increased values for q_2, implying that a greater fraction of present day warming is explained by warming on decadal timescales. The paleo constraint has a similar, but less dramatic effect - constraining the upper bound of the distribution for q_1 relative to the 'C,T' case.

S3 Sensitivity of scenario pathways to different historical constraints

The main paper considers scenarios in the case where only historical emissions and concentrations are known, but we can also consider the impact of different historical constraints on the pathways for 1.5C and 2.0C climate stabilization pathways. The temperature pathways are achievable, irrespective of the historical ensemble constraints used due to the large allowed negative emissions fluxes in the late 21st century (Figure S9), but the range of possible future emissions is dependent upon the prior assumptions (Figure S11) - the use of either the RWF or Paleo constraints tends to reduce the post-2050 negative emissions burden.

It is apparent that, as for the RCP2.6 case in Figure 1(b-e), there are large differences in the cumulative-emissions/temperature behavior for the different ensembles (Figure S12). Solutions with substantial hysteresis are possible with 'C,T', 'C,T,Heat' and 'C,T,Paleo' constraints - but not in the case of the 'C,T,RWF' constraint. Associated net 2100 cumulative carbon budgets for 1.5 and 2C stabilization also vary by prior - with significantly larger allowances when the RWF or Paleo constraints are employed.

The relationship between mid-century temperatures and late century carbon removal requirements, however, remains relatively robust irrespective of ensemble constraint (Figure S13), though expected mid-century warming for a given amount of 2020-2050 net emissions is reduced by 0.1-0.2K if the RWF or Paleo constraint is used (Figure S15). For example, a 2020-2050 budget of 100GtC produces a likely 2050 warming of 1.6K if 'C,T' constraints are used, and 1.45K if 'C,T,RWF is used'.

However, the 2050-2100 negative emission requirements are broadly similar for a given level of observed 2050 warming, irrespective of the constraint. For example, if observed warming in 2050 is 1.5C - this corresponds to allowable 2050-2100 emissions of -150 to +200GtC if C,T constraints are used, and 0 to +200GtC if C,T and RWF are used.

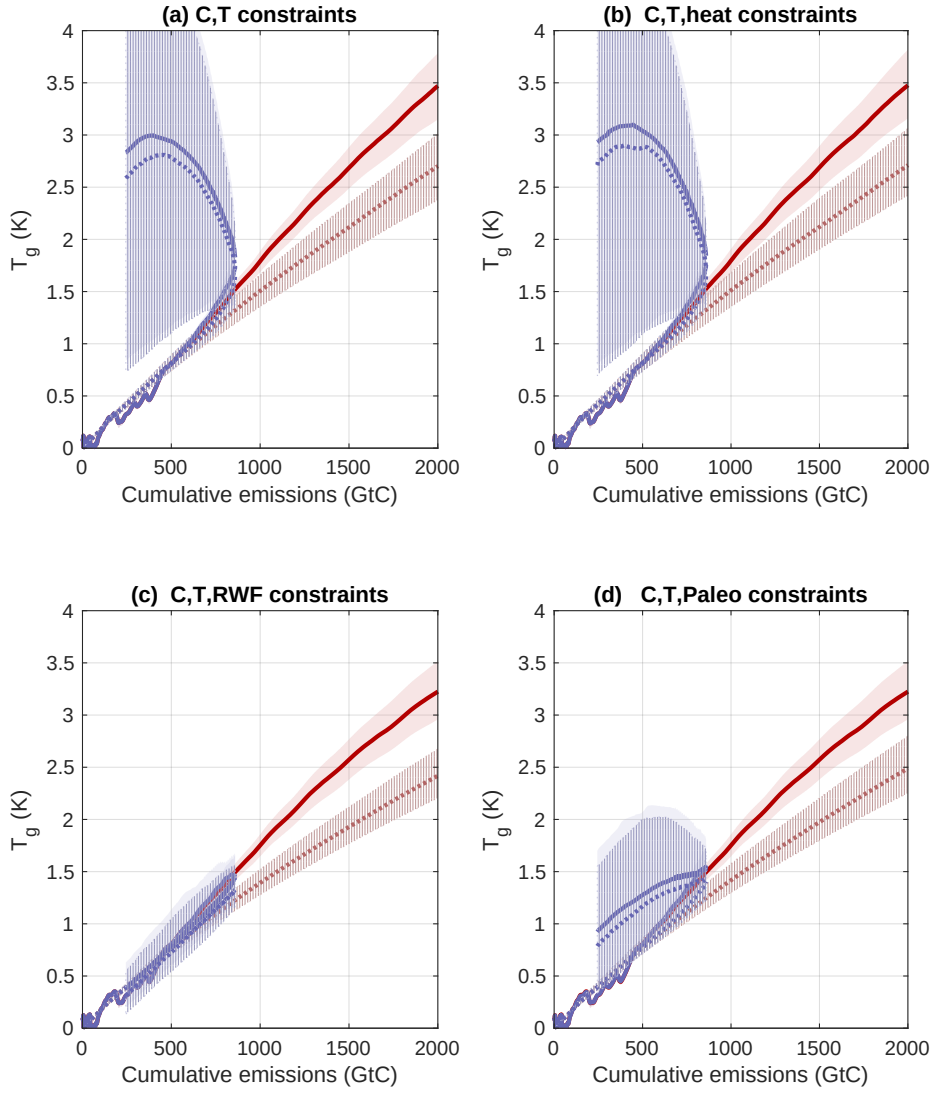

Figure S4. Illustration of the impact of non-CO2 forcers on model behaviour on temperature-cumulative emissions relationships, using different prior assumptions . Each subplot shows the 10-90th percentile ranges of projected response to cumulative emissions corresponding to Figure 1 in the main study. Solid/solid shade regions show the all forcing simulation, while hatched/dotted lines show the response of the same ensemble to a CO2-emissions only simulation, with all other forcings set to zero. RCP8.5/RCP2.6 are shown in red/blue respectively.

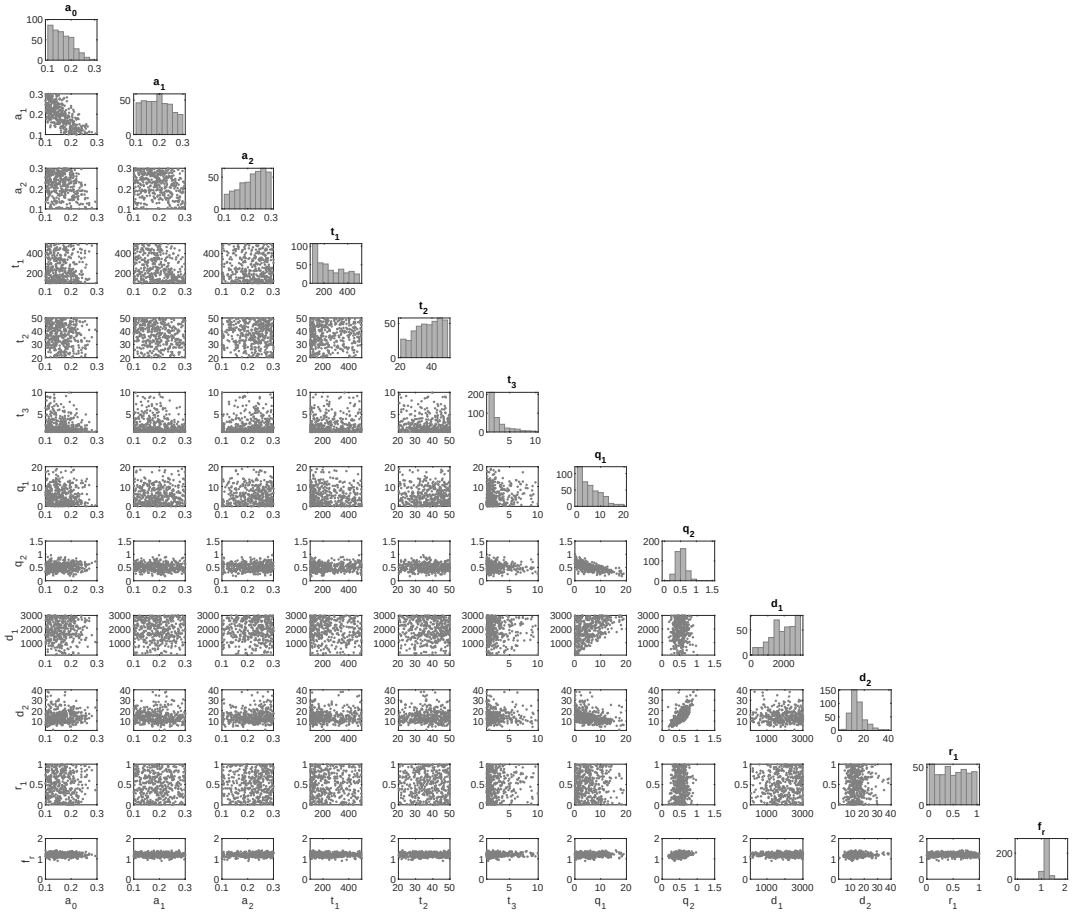

Figure S5. A 'corner-plot' showing pairwise posterior parameter distributions for models constrained using HadCRUT temperature anomalies from 1850-2016. Plots on the diagonal show parameter distributions for each of the parameters in Table 1 considered in the MCMC optimization only historical emissions and temperatures. Off-diagonal plots illustrate 2 dimensional distributions.

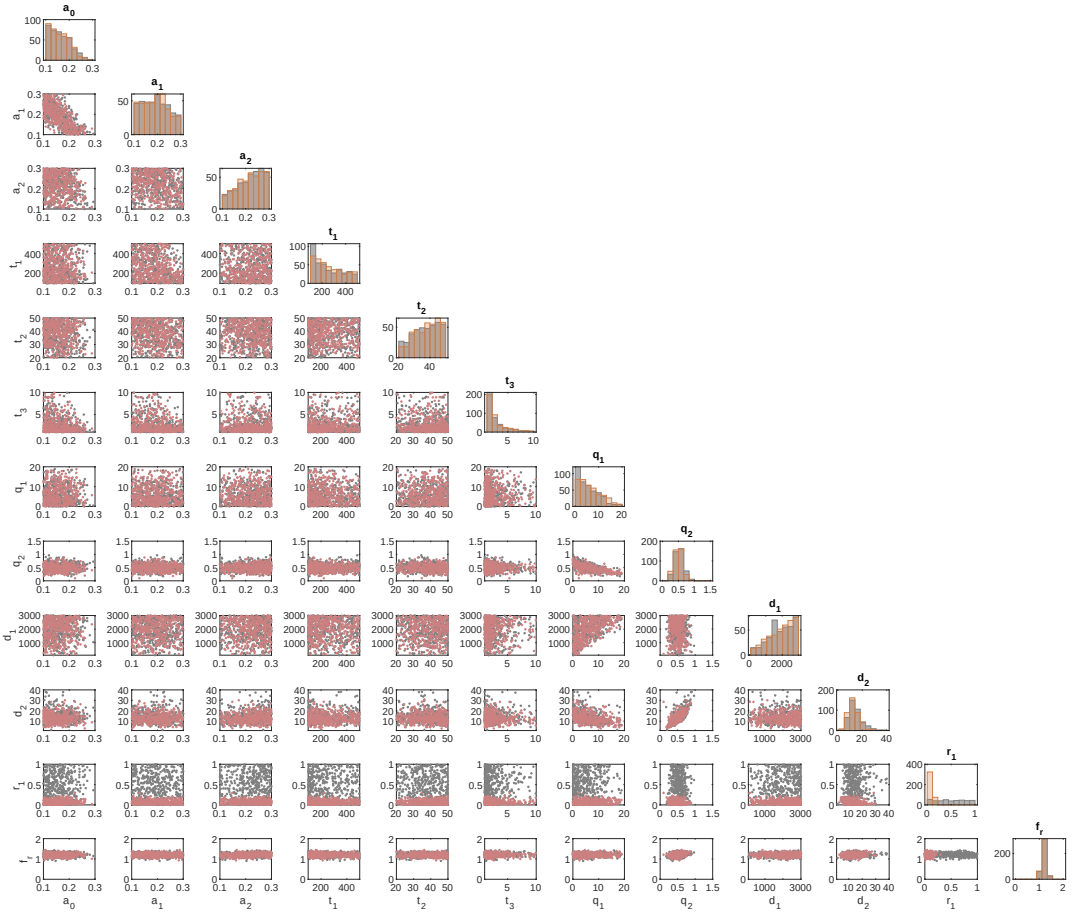

Figure S6. As for Figure S5, but with 'C,T' only constraints in gray and 'C,T and Heat' constraints i red.

.

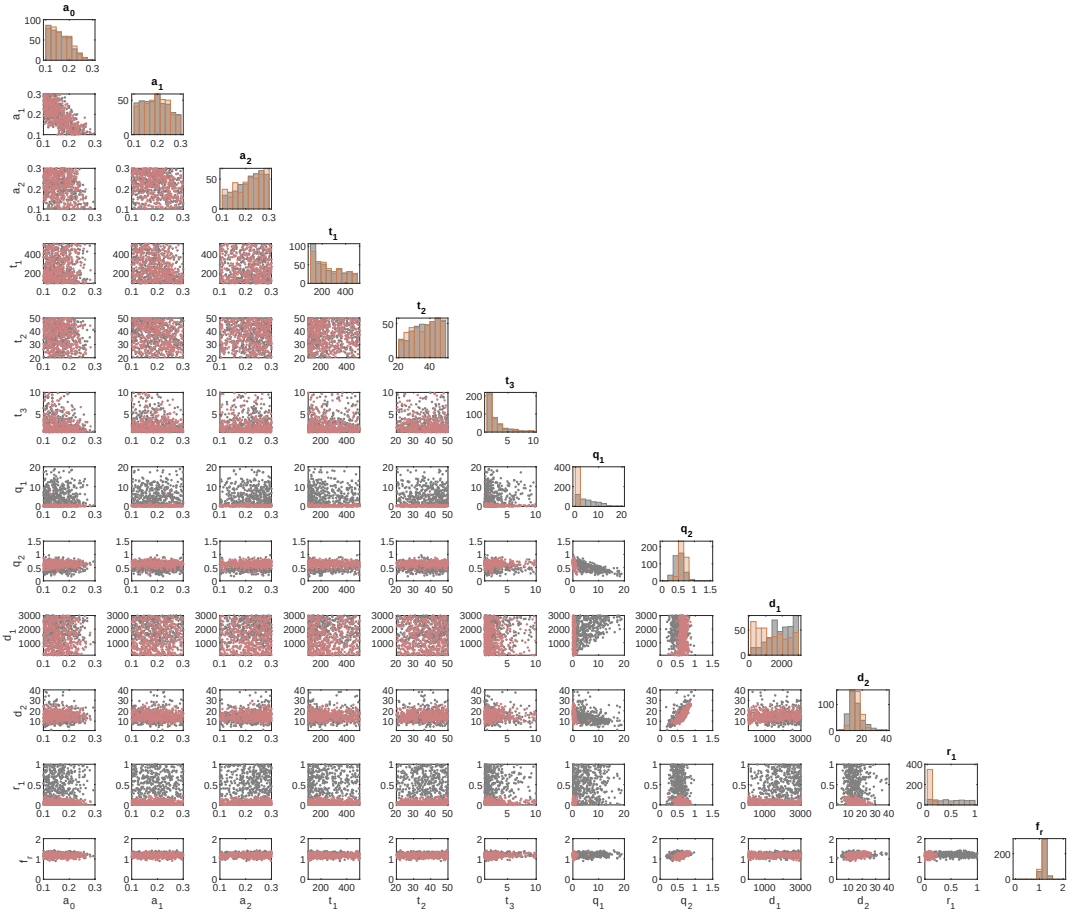

Figure S7. As for Figure S5, but with 'C,T' only constraints in gray and using 'C,T,RWF' constraints in red.

.

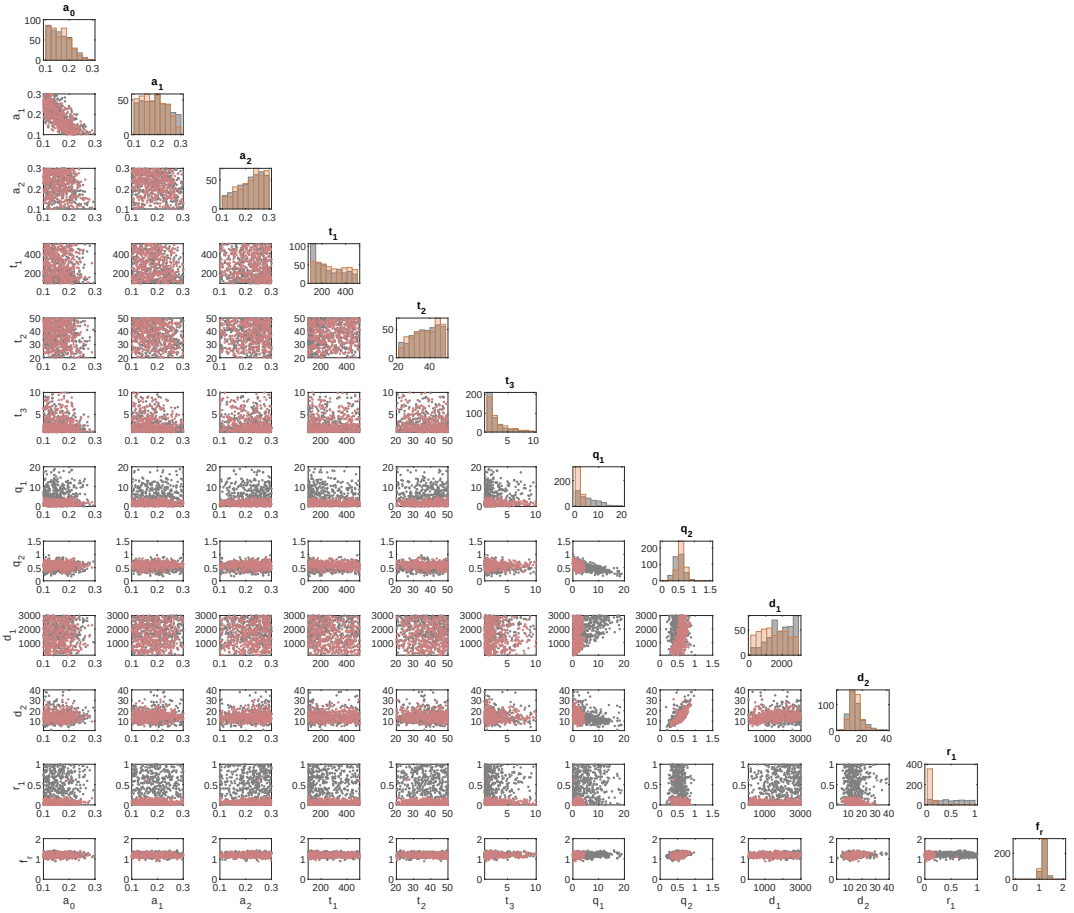

Figure S8. As for Figure S5, but with 'C,T' only constraints in gray and 'C,T,Paleo' constraints in red.

.

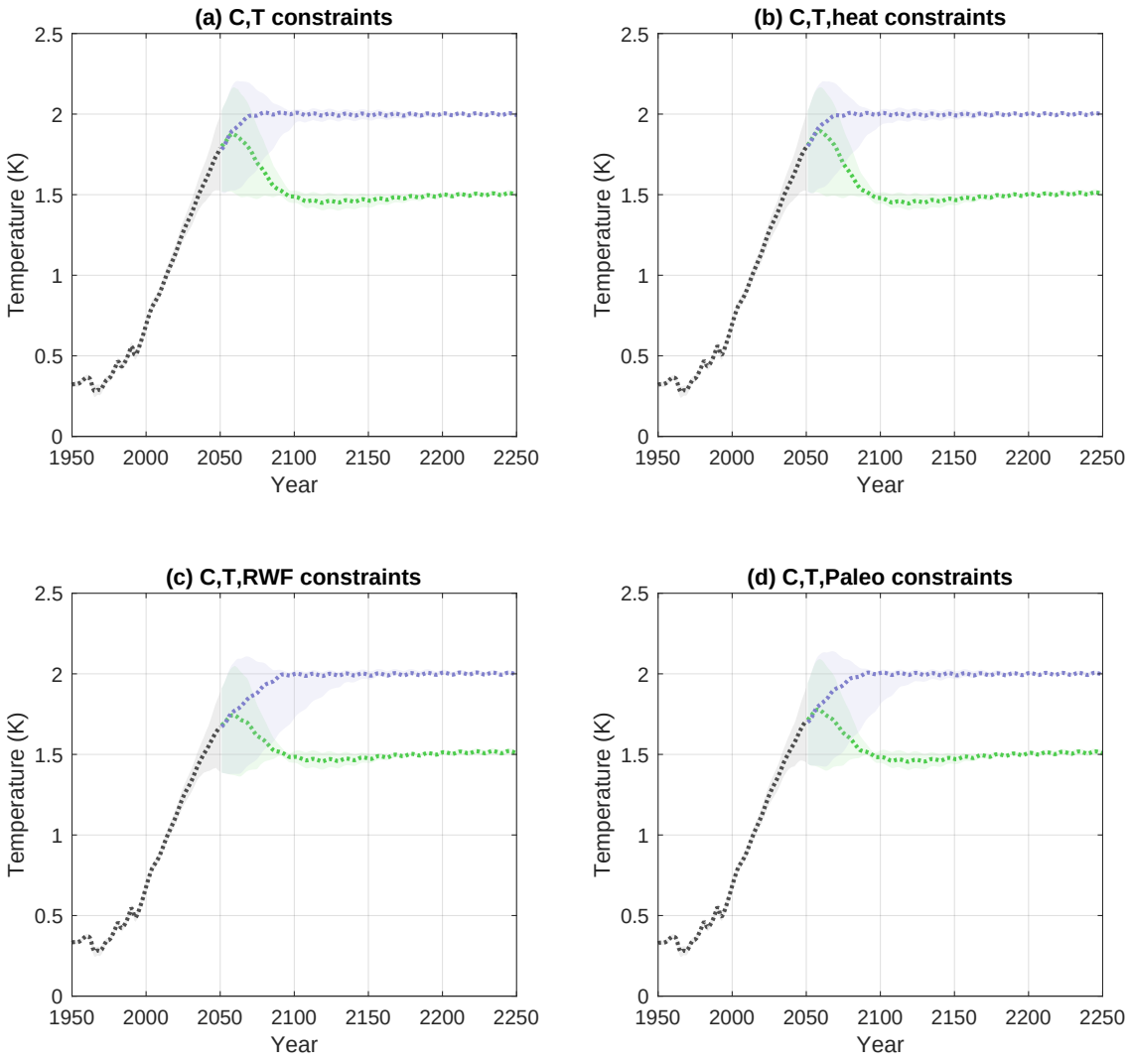

Figure S9. As for Figure 2(a), for each of the constraints considered in Figure 1(b-e).

.

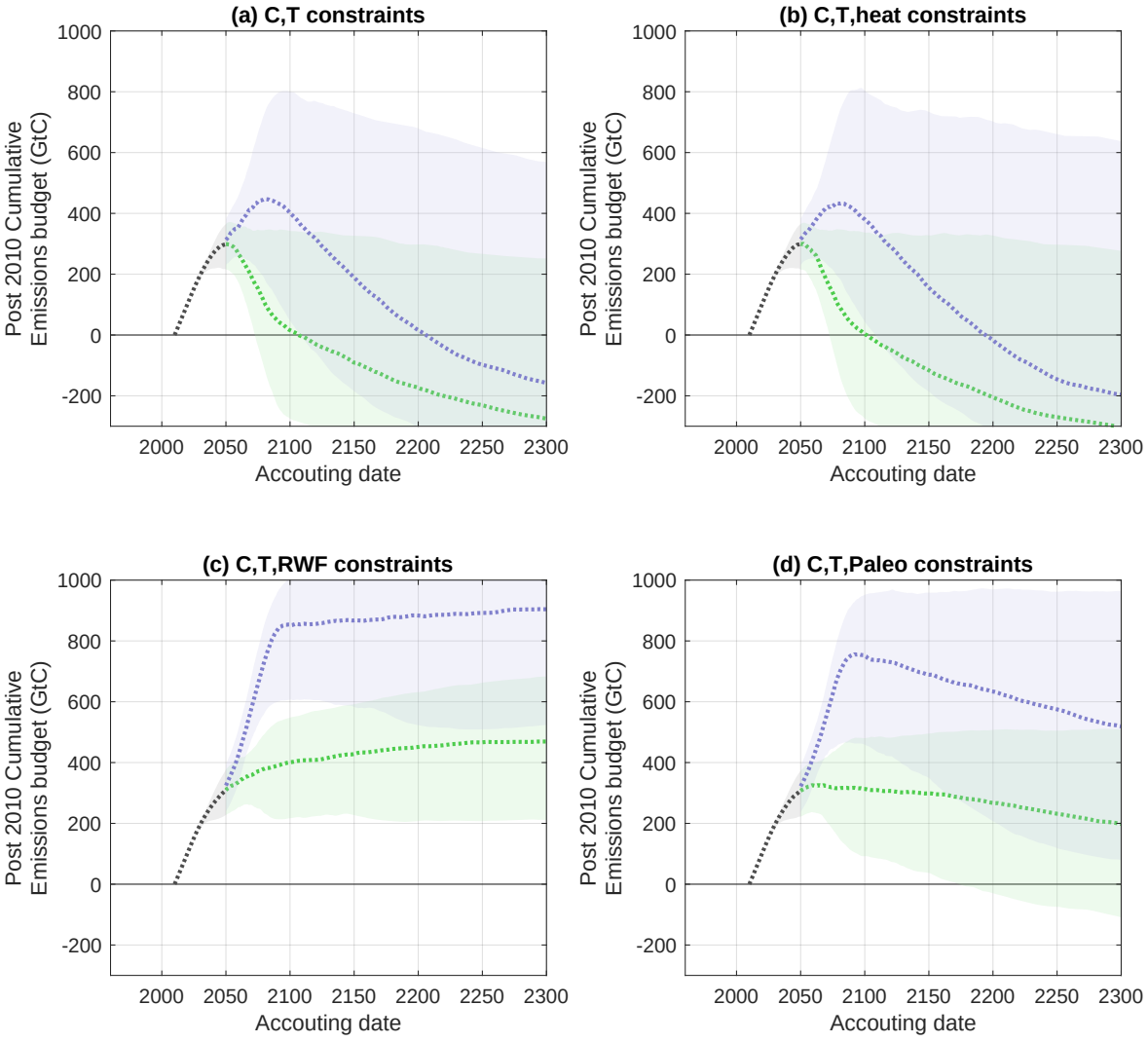

Figure S10. As for Figure 2(d), for each of the constraints considered in Figure 1(b-e).

.

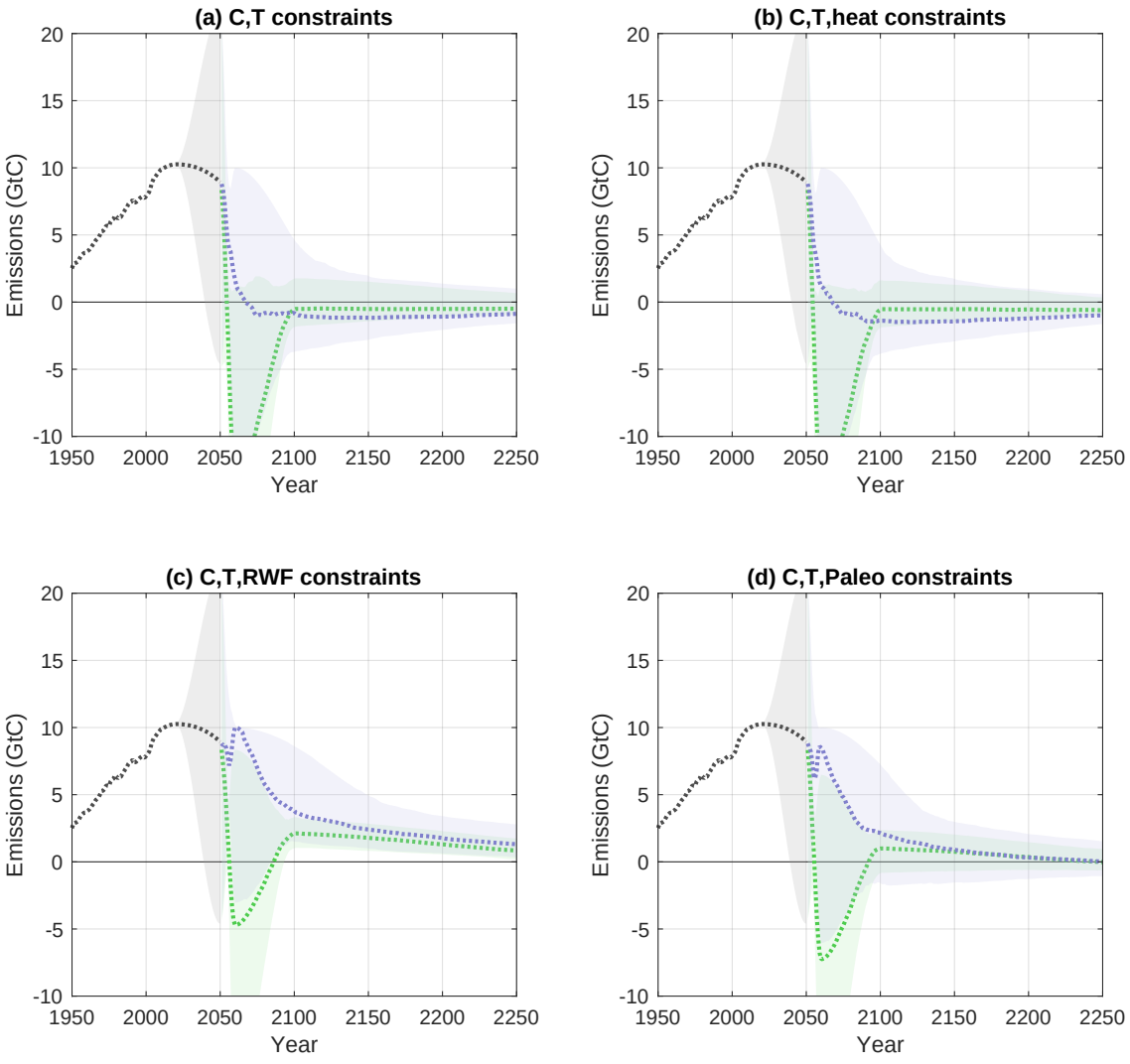

Figure S11. As for Figure 2(b), for each of the constraints considered in Figure 1(b-e).

.

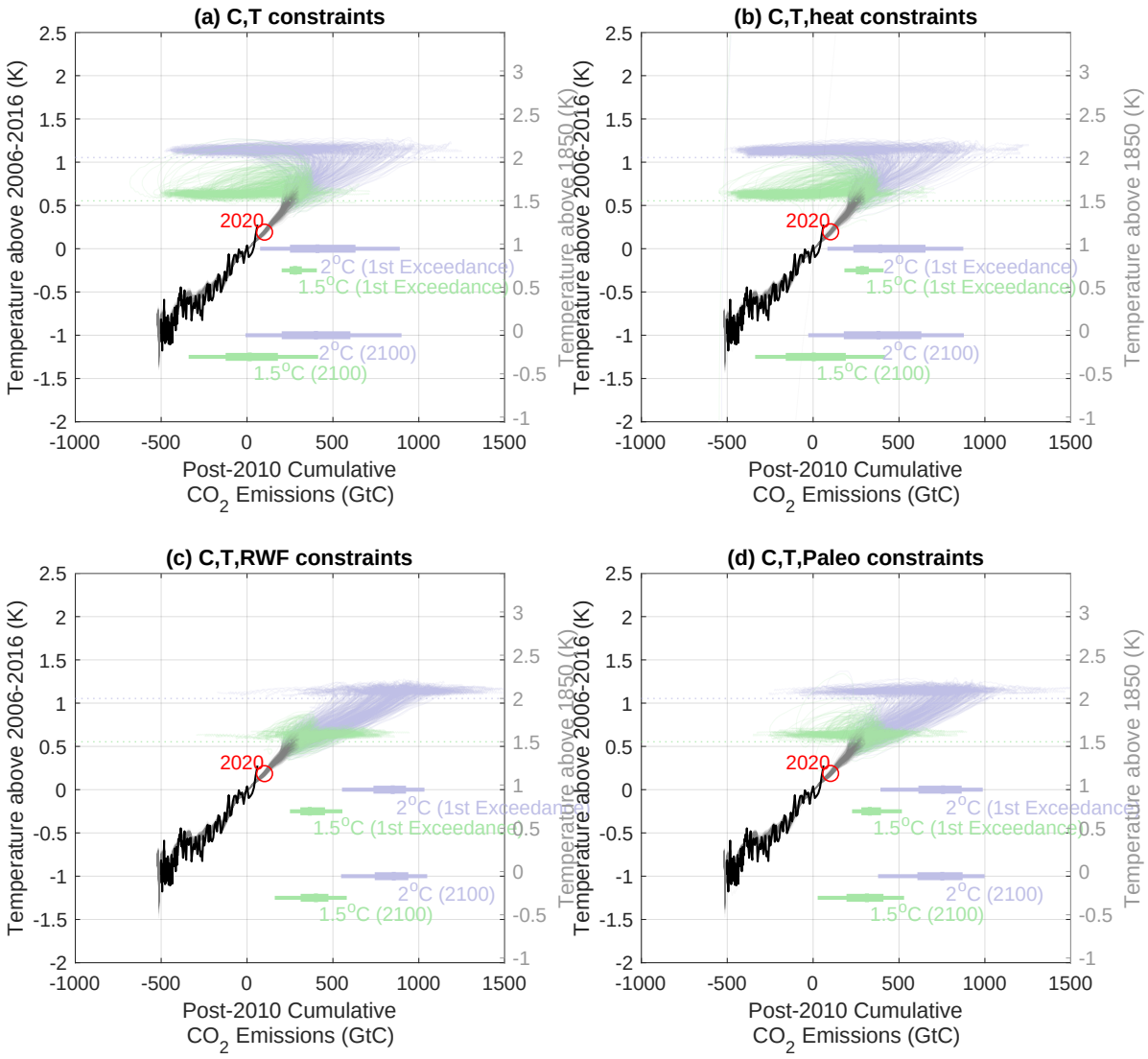

Figure S12. As for Figure 2(c), for each of the constraints considered in Figure 1(b-e).

.

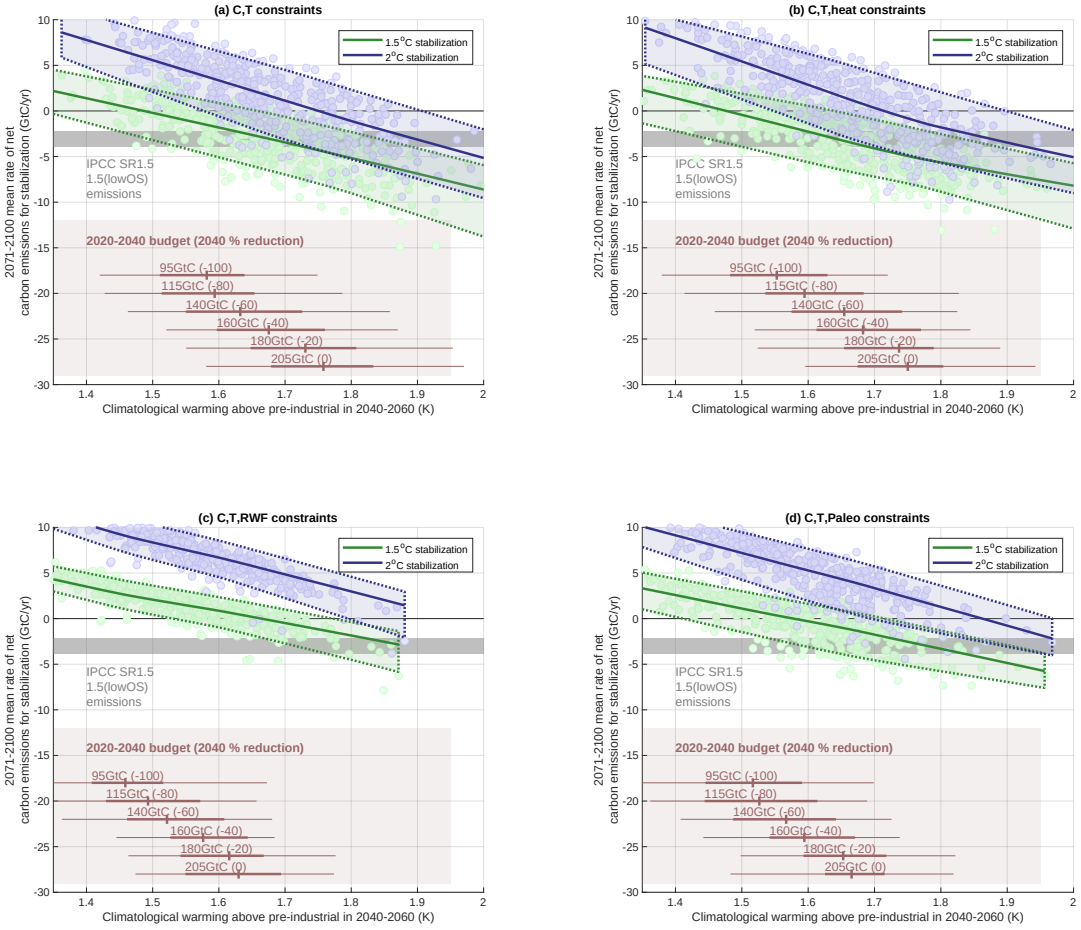

Figure S13. As for Figure 3(b), for each of the constraints considered in Figure 1(b-e).

.

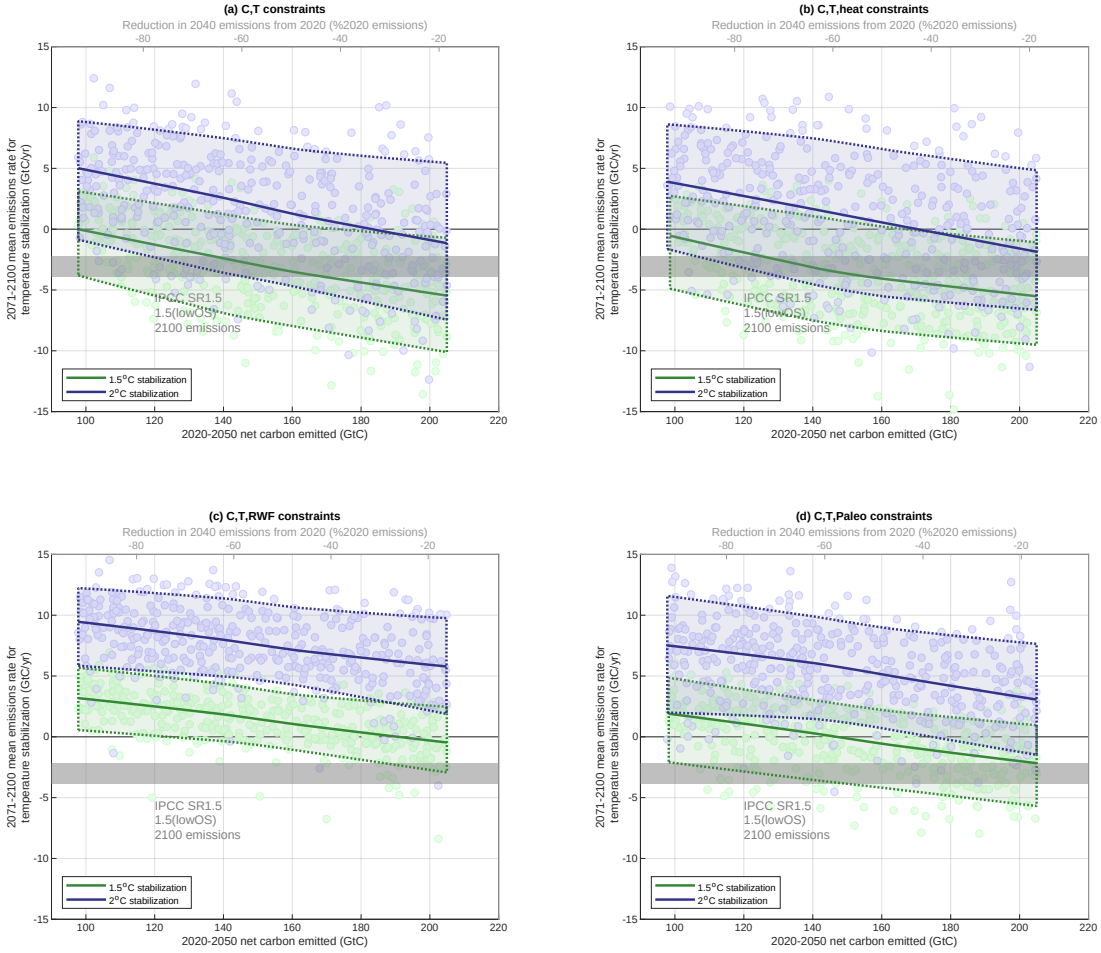

Figure S14. As for Figure 3(a), for each of the constraints considered in Figure 1(b-e).

.

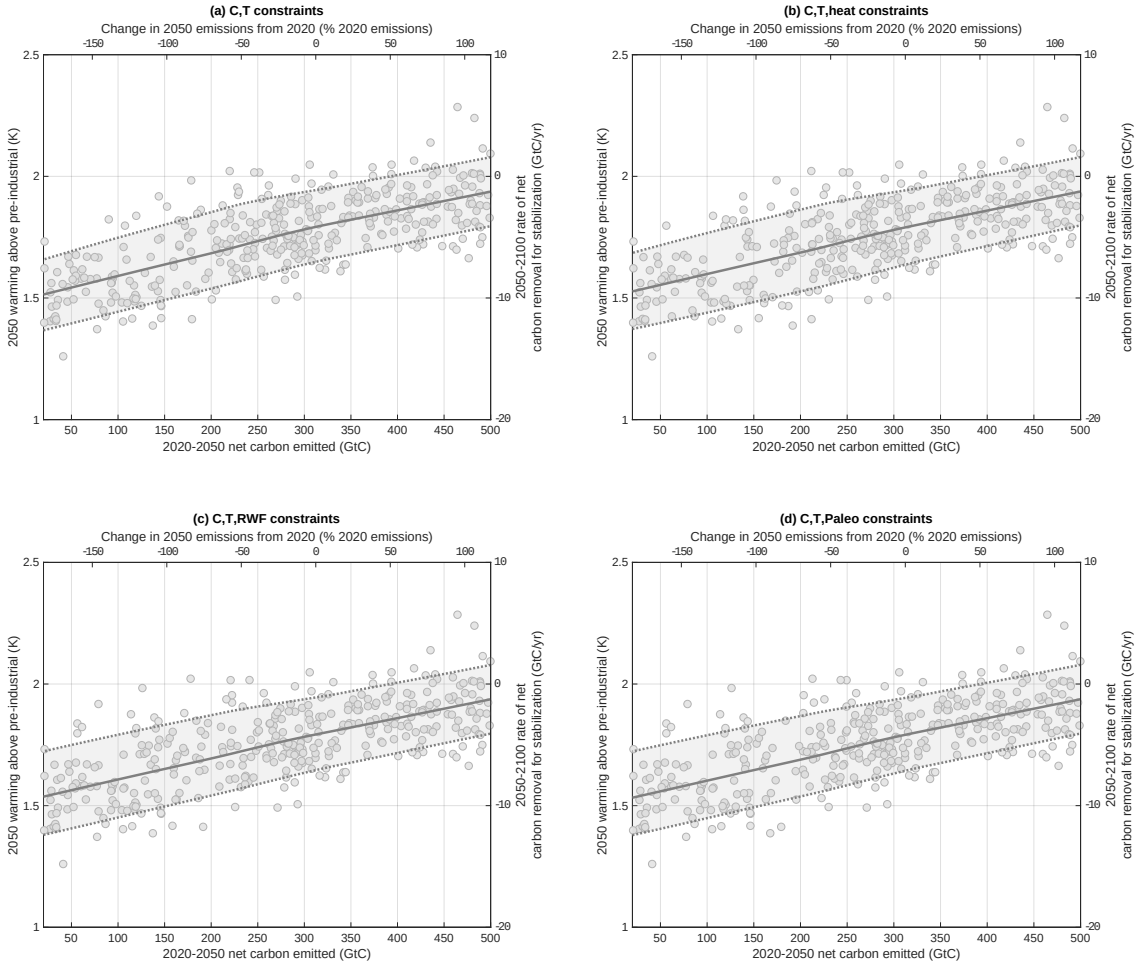

Figure S15. As for Figure 3(b), for each of the constraints considered in Figure 1(b-e).

.

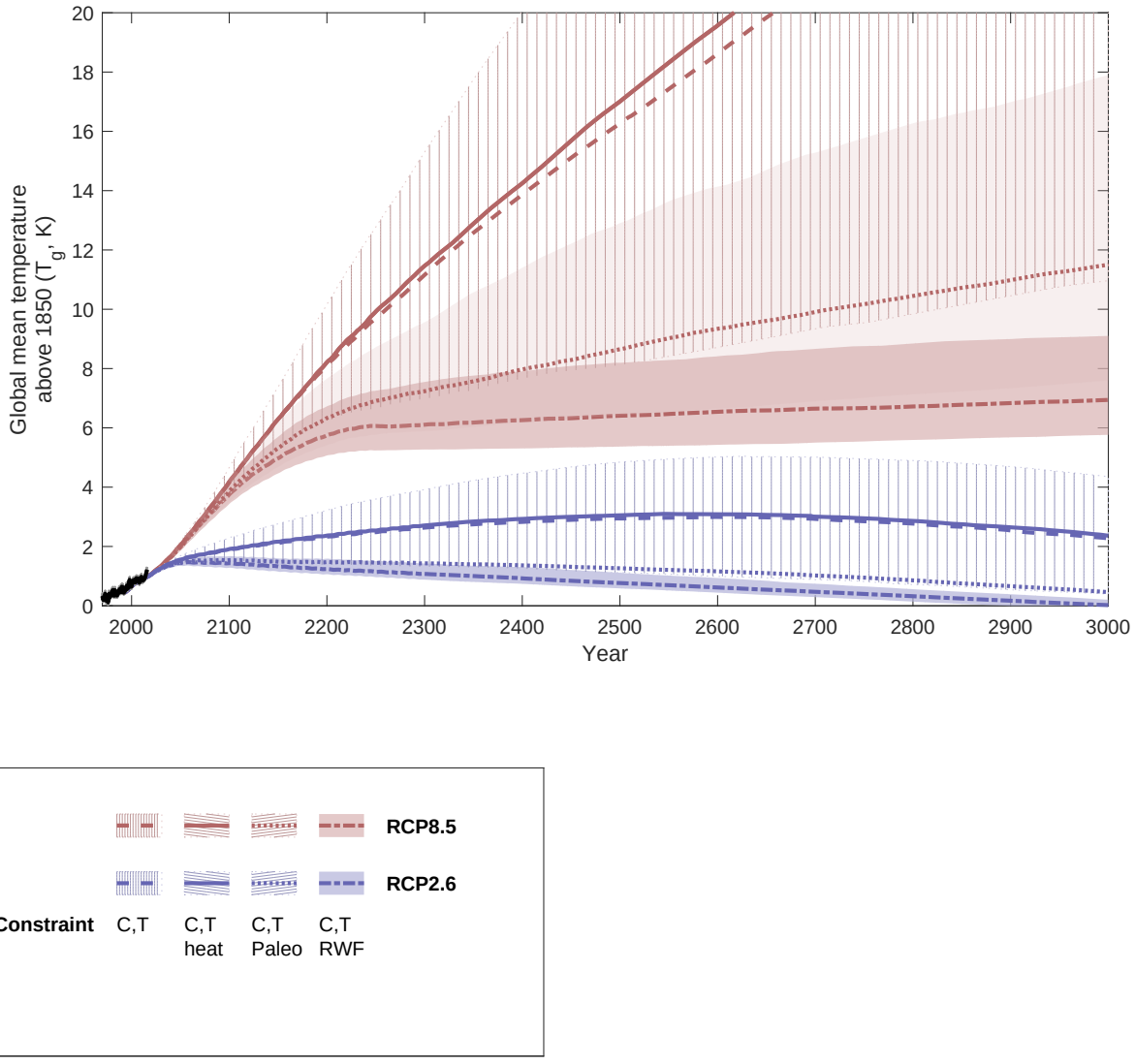

Figure S16. As for Figure 1(a), with the time axis showing millennial-scale evolution, with 2300 emissions remaining constant until the year 3000 in all cases.

.